8080 J. Med. Chem. 2010, 53, 8080–8088
DOI: 10.1021/jm1010012

Journal of Medicinal Chemistry Article

Virtual Screening to Identify Novel Antagonists for the G Protein-Coupled NK_3 Receptor

Werner J. Geldenhuys,[†] Stephanie R. Kuzenko,[‡] and Mark A. Simmons*[,†,‡]

[†]*Department of Pharmaceutical Sciences and* [‡]*Department of Integrative Medical Sciences, Northeastern Ohio Universities Colleges of Medicine and Pharmacy, Rootstown, Ohio 44272, United States*

Received July 23, 2010

The NK_3 subtype of tachykinin receptor is a G protein-coupled receptor that is a potential therapeutic target for several neurological diseases, including schizophrenia. In this study, we have screened compound databases for novel NK_3 receptor antagonists using a virtual screening protocol of similarity analysis. The lead compound for this study was the potent NK_3 antagonist talnetant. Compounds of the quinoline type found in the virtual screen were additionally evaluated in a comparative molecular field analysis model to predict activity a priori to testing in vitro. Selected members of this latter set were tested for their ability to inhibit ligand binding to the NK_3 receptor as well as to inhibit senktide-induced calcium responses in cells expressing the human NK_3 receptor. Two novel compounds were identified that inhibited NK_3 receptor agonist binding, with potencies in the nM range and antagonized NK_3 receptor-mediated increases in intracellular calcium. These results demonstrate the utility of similarity analysis in identifying novel antagonist ligands for neuropeptide receptors.

Introduction

The NK_3 receptor (NK_3R[a]) has recently been shown to be a viable drug target to treat several psychiatric diseases such as schizophrenia, depression, and anxiety.[1] The NK_3R is a member of the tachykinin peptide receptor family that is preferentially activated by the endogenous tachykinin peptide neurokinin B (NKB).[2] The role of NK_3 receptors in schizophrenia is thought to be mediated by dopamine.[3] Activation of the NK_3 receptor stimulates dopaminergic neurons to release dopamine, leading to high levels of occupation of D_2-receptors. Blockade of the NK_3R inhibits this release of dopamine. Because NK_3Rs are discretely localized in the central nervous system and because NK_3R antagonists are highly selective and do not bind to dopamine, serotonin, histamine, muscarinic cholinergic, or other receptors, their side effect profile should be more favorable than the multiacting receptor-targeted antipsychotics (MARTAs), the current primary therapy for schizophrenia. Additional support for the development of NK_3 antagonists for schizophrenia was obtained recently in a metatrial comparing the NK_3 antagonist osanetant and three other novel compounds, a serotonin $5\text{-}HT_{2A/2C}$ antagonist, a central cannabinoid CB_1 antagonist, and a neurotensin NTS_1 antagonist, to haloperidol.[4] The group receiving the NK_3 antagonist showed significant improvement in several measures of psychotic symptoms. In addition, the NK_3 antagonist was well-tolerated, with the NK_3 group having the highest percentage of patients who completed the study (43%), reinforcing the concept that their side effects are more tolerable compared to the MARTAs.

Two NK_3 antagonists, osanetant (SR-142801) and talnetant (SB-223412), have been tested in clinical trials (Figure 1). Both agents are small-molecule, nonpeptide antagonists that inhibit [^{125}I]-MePhe^7-NKB binding to the human NK_3R (hNK_3R) expressed in CHO cell membranes with K_is of ~1 nM.[5] In HEK-293 cells expressing the hNK_3R, talnetant inhibited the Ca^{2+} responses induced by 1 nM NKB with an IC_{50} of 16.6 nM and talnetant inhibited them with an IC_{50} of 6.1 nM.[6] Of interest to us is talnetant, a quinoline-type compound with high selectivity for the NK_3R and good oral bioavailability.[1,6]

In this study, we describe the identification of novel NK_3R antagonists discovered by the use of a virtual screening paradigm. Initially, we used talnetant as the template in a shape/electrostatic similarity analysis to identify compounds whose structures were consistent with NK_3 antagonist activity. Because similarity analysis usually has no biological predictive activity associated with it, a second tier of analysis was introduced. In this phase, chemotypes similar to talnetant, i.e. quinoline compounds, were passed on to a comparative molecular field analysis (CoMFA) model. This model was used to predict a priori NK_3 binding activity and therefore the value of testing the compound in biological assays. This method of analysis has led to the discovery of several new compounds that act as NK_3 antagonists in ligand binding and functional studies of the hNK_3R.

Results and Discussion

Because most virtual screening methods based on similarity screening are devoid of the ability to predict activity, a CoMFA model in addition to similarity analysis was used to evaluate the quinoline-type compounds identified in the initial virtual screen. This method has, to our knowledge, not been

*To whom correspondence should be addressed. Phone: +1-330-325-6525. Fax: +1-330-325-5912. E-mail: simmons@neoucom.edu.

[a] Abbreviations: CoMFA, comparative molecular field analysis; EC_{50}, the concentration of drug that produces a half-maximal response; hNK3R, human NK_3 receptor; IC_{50}, the concentration of drug that produces a half-maximal inhibition; MARTA, multiacting receptor-targeted antipsychotics; NK3R, NK_3 receptor; NKB, neurokinin B.

 Published on Web 11/03/2010

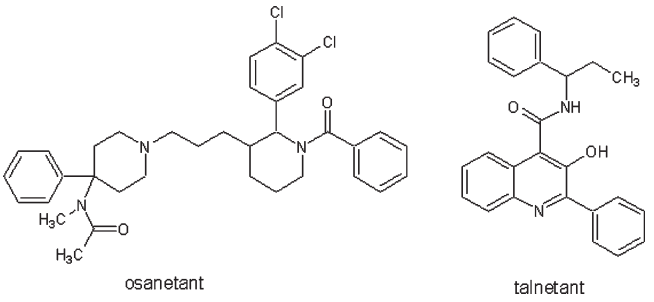

Figure 1. Chemical structures of NK_3 receptor antagonists that have been tested in clinical trials.

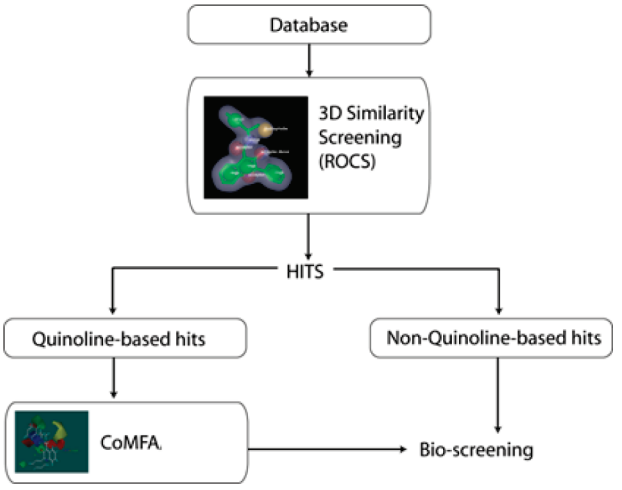

Figure 2. Workflow of the virtual screening for novel NK_3 receptor antagonists.

used before to identify NK_3R antagonists. Ligand-based virtual screening methods were employed in this study because the 3D structure of the human NK_3 receptor has not been established. The virtual screening workflow that was followed in this study is shown in Figure 2.

After our initial screen, we focused on companies which had compounds in stock that were available for purchase. Many of the chemical companies have limited stocks of the compounds that they synthesize for their libraries. We validated both the first step of the virtual screen, the similarity analysis, as well as the second step in the process, the CoMFA model. To validate the similarity analysis, we used the validation method of ROCS 3.0, where a set of known active compounds are screened against the target compound (talnetant in this case) and also against a set of decoy compounds. We used a combination of shape and color in the virtual screening method.

Initially, we only aligned the compounds using the shape ranking method, which did not lead to very good alignments, as indicated by low cross-validated q^2 values (data not shown). By adding the color flag to the shape ranking method, the reactive groups (e.g., NH_2, OH) were better aligned for CoMFA analysis and were used as such in this study. Figure 3 shows the alignment of the quinoline compounds used in this study. Using talnetant as the query molecule, the aligned molecules were then used in the CoMFA analysis. Similar to the first step in the virtual screening protocol, we validated our CoMFA model by utilizing a test set which was not used to develop the original CoMFA model. The results of the CoMFA analysis are shown in Table 1. The contour maps of the CoMFA steric and electrostatic fields are shown in Figure 4A, with talnetant

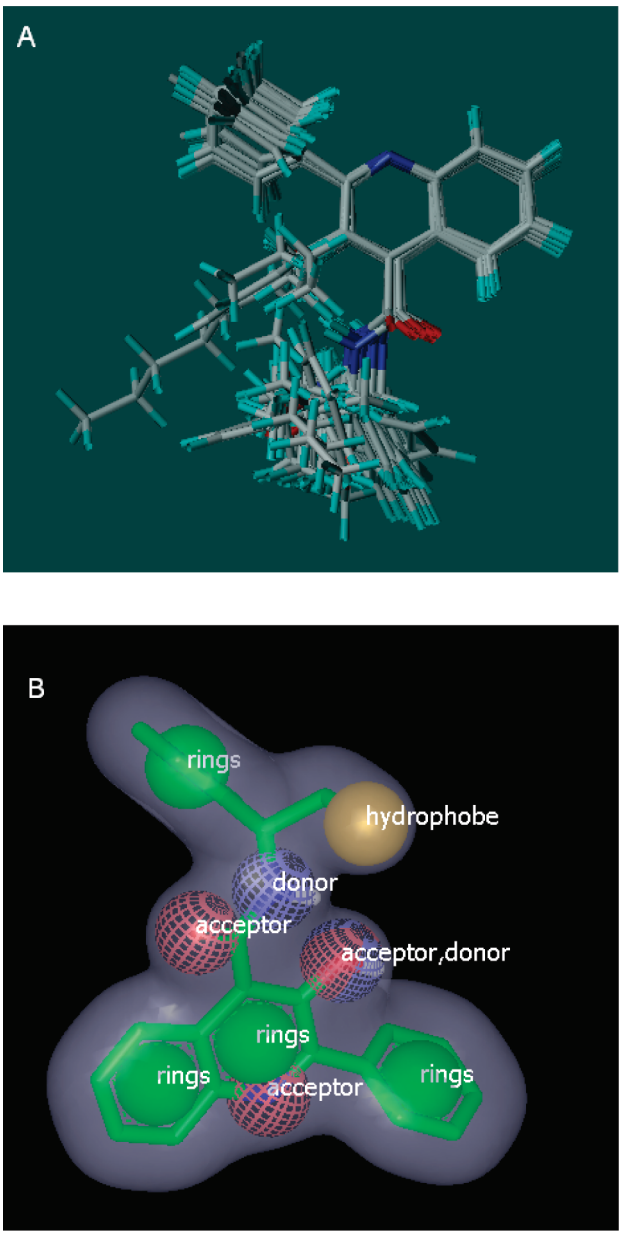

Figure 3. (A) Alignment of active compounds used in the 3D-QSAR studies. Talnetant was used as query in ROCS to automatically align the compounds for use in the CoMFA models. (B) The major color characteristics used in the query, in addition to shape searching.

shown within the contour maps as reference and the results from the PLS shown in Figure 4B. For the CoMFA model, the cross-validated PLS q^2 value was 0.49, suggesting it to be a good predictive and descriptive model, where $q^2 > 0.3$ is considered to be significant.[7] The non-cross-validated PLS gave a value of 0.886 (Table 2).

In the CoMFA maps, the green maps indicate regions or areas where sterically bulky groups are favored and yellow areas where big bulky groups are disfavored, respectively. As can be seen in Figure 4A, large regions of green contour can be seen near the ethyl moiety of talnetant, as well as near the hydroxyl group on the quinoline ring and at the *meta*-position of the aromatic ring, which is attached to the quinoline ring system. A yellow area is found close to the ethyl moiety on the other side of the green map. This suggests a limit to sterically increasing bulk in this direction, and that if the group becomes too large, this area in the receptor will not allow for optimum

Table 1. Results from the CoMFA Analysis[a]

						fraction	
Q^2	SEP	NC	R^2	SEE	F	steric	electrostatic
0.490	0.775	3	0.886	0.367	59.30	0.490	0.510

[a] Q^2 is the cross-validated regression correlation coefficient; R^2 is the non-cross-validated regression coefficient; SEP is standard error of prediction; NC is number of components used in PLS analysis; SEE is standard error of estimate; F is the Fischer ratio.

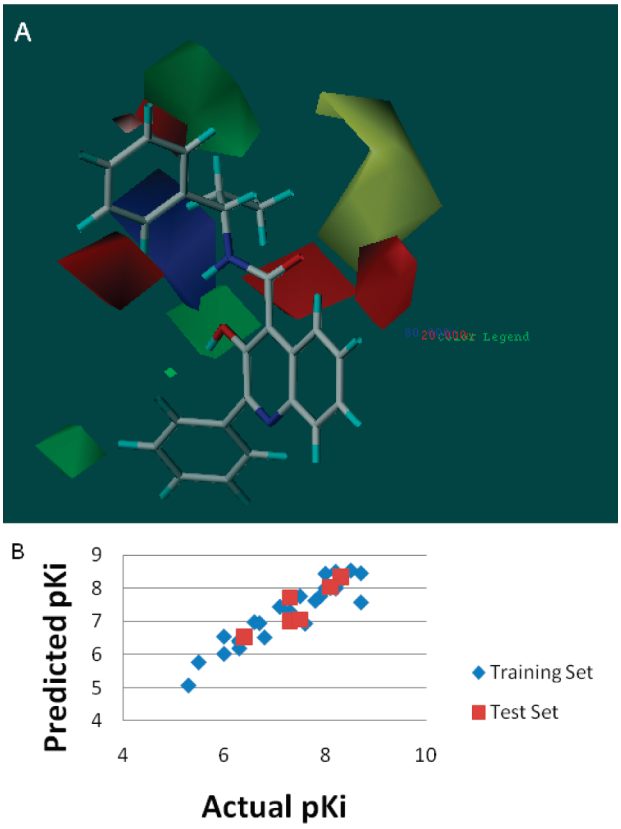

Figure 4. (A) CoMFA model with the steric and electrostatic fields shown. Green steric maps show areas where steric bulk would likely increase activity, and yellow shows sterically disfavored areas. The blue areas show areas were positive charge would likely increase activity, and the red areas where negative charge would likely increase activity. Talnetant is shown for orientation purposes. (B) Correlation between actual and predicted CoMFA for training and test set. The test set r^2 was 0.8076.

binding. Although contour maps of CoMFA cannot be used to act as a "receptor map", this may suggest that this area may sterically aid in aligning the quinoline compounds in the NK_3 binding pocket. The green/yellow areas surrounding the ethyl moiety of talnetant also explains the increase in activity of the cyclopropyl compounds (**9**−**14**) when compared to compounds **24**−**27**, where *n*-alkane side chains are attached. Second, the smaller green contour near the hydroxyl moiety attached to the quinoline ring of talnetant explains the increase in activity from talnetant (pK_i = 8.7) to that of compound **28**, where the hydroxyl group is replaced with a hydrogen (pK_i = 6.4). Similarly, the green contour map at the *meta*-position on the aromatic ring moiety attached to the quinoline of talnetant seems to favor substitution. The inhibitors with a *meta*-substitution as compared to *ortho* or *para* seem to be better in general.

The blue and red CoMFA contour maps indicate areas where positive and negative charges are favored. As can be seen in Figure 4A, the blue contour maps are near the amino group of talnetant. This suggests that positively charged groups will likely increase activity of inhibitors. In contrast, a red contour map is seen near the ketone moiety of talnetant, suggesting that this area of the quinoline antagonists favors negatively charged groups. As suggested by the group of Tropsha, we also did a test set validation.[8] To validate the CoMFA model, we used a test set of compound which was not used to develop the CoMFA model. As can be seen from Figure 4B and in Table 3, the CoMFA model was able to predict the test set pK_i values for NK_3 binding with an r^2 of 0.8076, suggesting that the CoMFA model is able to satisfactory predict the activity of other quinoline compounds at the NK_3 receptor, specifically assessing if activity will be below a 10 μM cutoff, which we deemed as qualifier for testing in vitro.

After virtual screening, the hit compounds could be roughly divided into two sets of compounds based on chemical scaffold (Table 4). As can be expected from a similarity analysis type virtual screen, quinoline type compounds were identified as well as other compounds which have a different scaffold than the quinoline type compounds. The quinoline-type compounds were then screened using the 3D-QSAR method,

Table 2. Biological Values Used in This Study (pK_is from refs 6,9) and Results from the 3D-QSAR Which Predicts the Activity of Each Compound

		CoMFA	
compd	pK_i	predicted	residual
32	8.7	8.46	−0.24
8	7.5	7.77	0.27
9	6	6.03	0.03
10	6.3	6.43	0.13
11	6.3	6.20	−0.10
12	6	6.55	0.55
13	6.6	6.99	0.39
16	7.1	7.45	0.35
17	6.8	6.53	−0.27
18	5.3	5.08	−0.22
19	5.5	5.78	0.28
20	7.6	6.95	−0.65
21	6.7	6.96	0.26
23	6.3	6.39	0.09
24	8	8.02	0.02
25	8.2	8.01	−0.19
26	7.9	7.77	−0.13
27	7.8	7.63	−0.17
29	7.3	7.31	0.01
30	8.2	8.08	−0.13
31	8.6	7.59	−1.01
7	8.2	8.51	0.31
5	8.5	8.55	0.05
4	8	8.45	0.45
3	8.3	8.37	0.07
1	8.4	8.42	0.02

Table 3. Results from the Test Sets of Compounds As Predicted Using the 3D-QSAR Models

		CoMFA	
compd	pK_i	predicted	residual
6	8.30	8.33	*0.03*
28	7.30	7.72	*0.42*
22	6.40	6.54	*0.14*
15	7.30	7.02	*-0.28*
14	7.50	7.06	*-0.44*
2	8.10	8.04	*-0.06*

Table 4. Compounds Which Were Retrieved from the Virtual Screening and Their Ability to Inhibit hNK_3R-Mediated responses

Structure	Compound Number	Antagonism of hNK_3R- mediated calcium response (% inhibition)	Structure	Compound Number	Antagonism of hNK_3R- mediated calcium response (% inhibition)
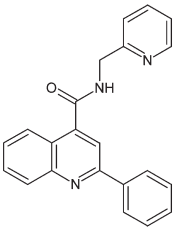	**33**	17	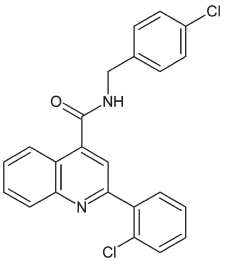	**39**	14
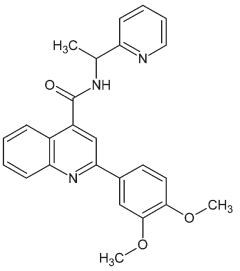	**34**	16	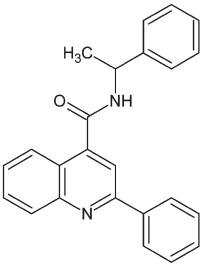	**40**	61
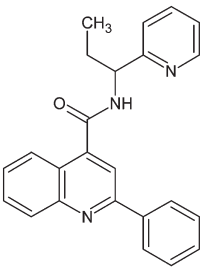	**35**	82	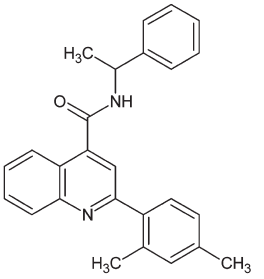	**41**	18
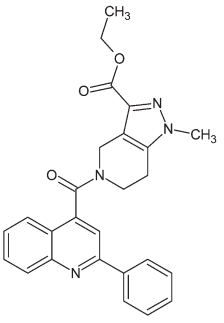	**36**	8	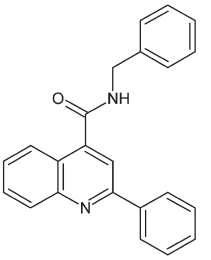	**42**	30
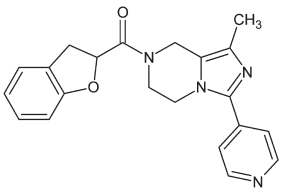	**37**	6	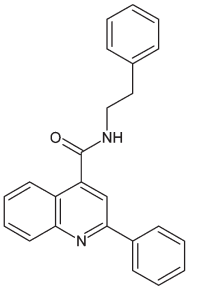	**43**	54
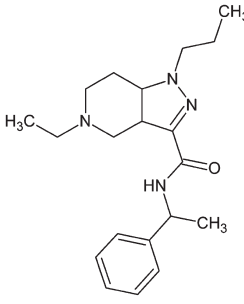	**38**	6	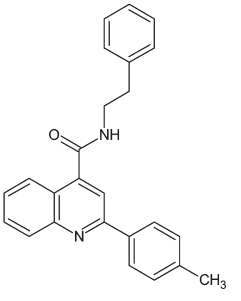	**44**	17

Table 4. Continued

Structure	Compound Number	Antagonism of hNK_3R- mediated calcium response (% inhibition)	Structure	Compound Number	Antagonism of hNK_3R- mediated calcium response (% inhibition)
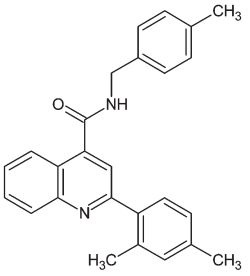	**45**	9	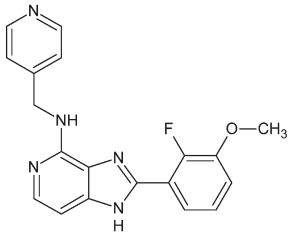	**49**	39
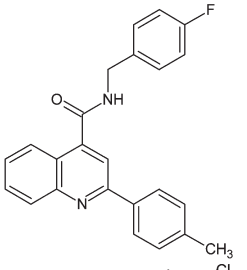	**46**	7	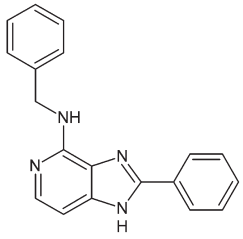	**50**	42
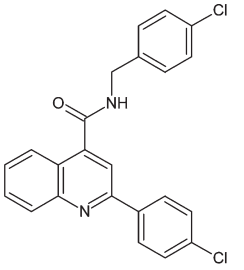	**47**	13	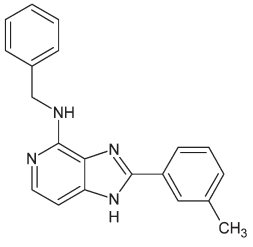	**51**	40
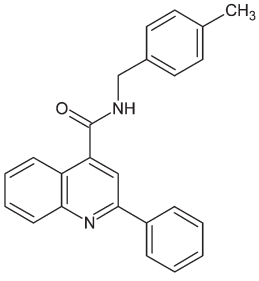	**48**	21			

which suggested them to be active NK_3 antagonists at 10 μM or less.

Receptor Binding and Antagonist Activity. The quinoline-type compounds were able to attenuate senktide-induced calcium responses of CHO cells expressing human NK_3Rs. For initial screening, cells were incubated with each compound at a concentration of 50 μM for 10 min. The response to senktide (200 nM) was then measured and compared to senktide responses in the absence of antagonist compound. The percent inhibition of the senktide response by 17 compounds tested in this assay is shown in Table 4. Two compounds, **40** and **35**, were found to be most effective and were chosen for further study.

Both compounds **40** and **35** effectively competed with ^{125}I-MePhe^7-NKB binding to the human NK_3R, as shown in Figure 5, with IC_{50}s in the nM range. Compound **35** was more potent.

The compounds were tested with respect to their ability to inhibit the response to two different NK_3R agonists, MePhe^7-NKB and senktide. MePhe^7-NKB is an NKB analogue with the Val at the seventh position substituted by a methylated Phe.[9] Senktide is an analogue of a fragment of NKB. It consists of NKB(4−10) with the Asp at position 4 succinylated, the Phe at position 6 deleted, and the Val at the seventh position substituted by a methylated Phe. Compared to NKB, MePhe^7-NKB and senktide have a higher selectivity for the NK_3 receptor over NK_1 and NK_2 receptors. They are the most commonly used agonists for studying NK_3R-mediated responses.

The ability of compounds **40** and **35** to antagonize the responses of the human NK_3R to MePhe^7-NKB is shown in Figure 6A and to senktide is shown in Figure 6B.

These data show that both of the novel compounds, **40** and **35**, are NK_3R antagonists. Both compounds are effective

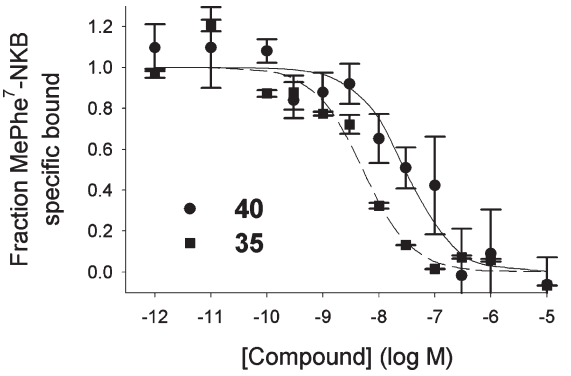

Figure 5. Effect of compounds identified from virtual screening on ^{125}I-MePhe^7-NKB binding to the human NK_3R. (●) Fraction of specific ^{125}I-MePhe^7-NKB binding in the presence of increasing concentrations of **40**; the IC_{50} for this compound is 33.5 nM. (■) Fraction of specific ^{125}I-MePhe^7-NKB binding in the presence of increasing concentrations of **35**; the IC_{50} for this compound is 5.2 nM.

blockers of ligand binding and functional responses of NK_3R agonists. The relative potencies of the two agents are conserved in all three assays, with compound **35** being more potent.

Conclusion

The NK_3 receptor is a potential drug target for various CNS diseases, including schizophrenia. In this paper, we have used virtual screening based on sequential similarity analysis followed by CoMFA to identify novel compounds from the ZINC database.[10] The inclusion of the CoMFA model provided a second layer of screening, whereby biological activity could be predicted. Because the NK_3R has not been crystallized, we used similarity searching software as well as 3D-QSAR to identify possible new lead compounds. Although 3D-QSAR techniques such as CoMFA are generally not regarded as useful in virtual screening, we were able to successfully use it in an automated fashion in sequence with ROCS which aligned quinoline type compounds. The results indicate that this virtual screening method can be successfully used in mining NK_3 antagonists.

Experimental Section

Chemicals. Buffer chemicals used for receptor binding and functional studies were obtained from Fisher Scientific, Pittsburgh, PA, or Sigma-Aldrich, St. Louis, MO. α-MEM for cell culture was purchased from Mediatech, Inc., Manassas, VA. Fluo 4-AM was purchased from Invitrogen-Molecular Probes, Eugene, OR, and Pluronic F-127 from Texas Fluorescence Laboratories, Austin, TX. [^{125}I]-MePhe^7-NKB, specific activity 2200 Ci/mmol, was purchased from PerkinElmer, Boston, MA. The hit compounds found in the virtual screen, were purchased from Chembridge, San Diego, CA, and BioFocus, San Francisco, CA, as powders, and were all >98% pure as verified by HPLC by the vendors. Compound stocks at a concentration of 50 mM were prepared in dimethyl sulfoxide (≥99.5% pure by gas chromatography).

Virtual Screen Work Flow. Similarity Analysis. The similarity analysis was performed using the software suite from Openeye (Santa Fe, NM, USA). Talnetant was used a lead compound in the similarity virtual screening program ROCS 2.4.1 and 3.0, where version 3.0 was used to validate the "hit-rate" (with a build in function within the GUI interface). The lead compound used in this study is talnetant, which was sketched in SYBYL X (Tripos, St Louis MO), and energy minimized with termination criterion of 0.001 kcal/mol, for 1000 iterations, using the MMFF94s force field, which is parametrized for small organic molecules.

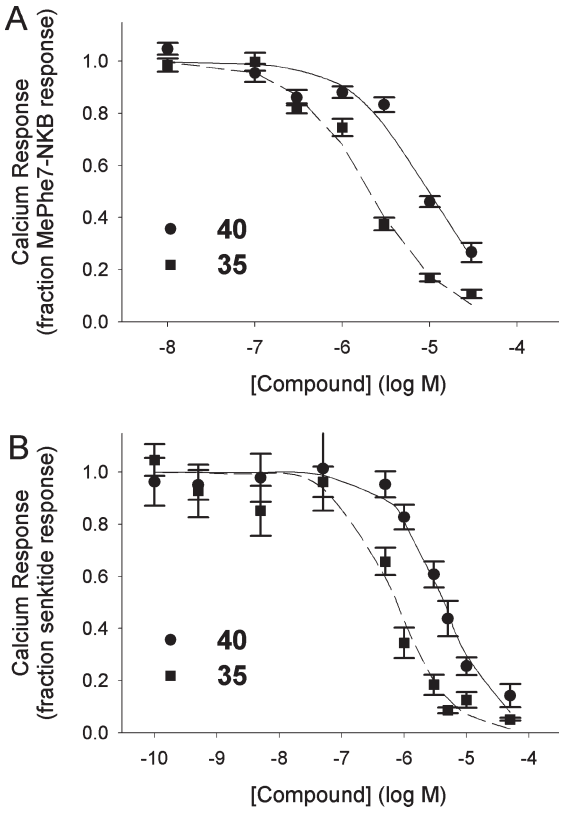

Figure 6. Effect of compounds identified from virtual screening on calcium responses of hNK_3R-expressing CHO cells produced by NK_3R agonists. (A) (●) Response to MePhe^7-NKB (50 nM) in the presence of increasing concentrations of **40**; the IC_{50} = 9.9 μM. (■) Response to MePh^7-NKB (50 nM) in the presence of increasing concentrations of **35**; The IC_{50} = 1.4 μM. (B) (●) Response to senktide (200 nM) in the presence of increasing concentrations of **40**; the IC_{50} = 2.2 μM. (■) Response to senktide (200 nM) in the presence of increasing concentrations of **35**; the IC_{50} = 0.9 μM.

Additionally, compounds used for the 3D-QSAR model (Table 5) development in this study were drawn using Marvin Sketch 5.2 (ChemAxon) in 2D and optimized in 3D initially using Marvin Sketch. The compounds were then combined into a single SDF file using Instant JChem, a database cheminformatics program (ChemAxon). This SDF file was then used by OMEGA (Openeye), which generates multiple conformers of each compound. ROCS 2.4.1 (command-line mode) and 3.0 (graphical-user interface mode) software from Openeye using the RANKBY COMBO flags which optimizes both shape overlay and chemical (color) overlay of the conformers generated by OMEGA of each compound in the training and test sets to that of the minimum energy conformation of talnetant. We aligned the training and test set compounds used in the CoMFA model, with ROCS as well, as it expedited the otherwise manual process in our case; the process is also more efficient using ROCS than the DATABASE ALIGN routine in SYBYL in our hands. Initially, we used only the shape overlay (Tanimoto scoring) but found that important reactive hydrogen-bond donor/acceptor pairs were not always necessarily overlaid, after which we added the COLOR flag to the search. Additionally, to test the virtual screening process, we used the Schrodinger decoy set of 1000 compounds as inactives. The known active compounds of Table 5 were ranked as well as the 1000 compounds in the decoy set. Using the validation module in ROCS 3.0, we looked at the ability of ROCS to rank the know actives at the top of the list as compared to the inactive compounds.

The resulting overlay of compounds shown in Figure 3 was then used for the CoMFA analysis in both the training and testing phases. Nonquinoline type compounds found were

Table 5. Structures of NK_3 Receptor Antagonists Used to Develop the CoMFA Models and Their Previously Determined K_is[a] [6,9]

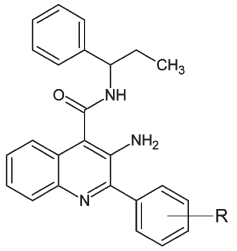

Cmpd	R	pK_i (M)
1	*m*-F	8.4
2	*p*-F	8.1

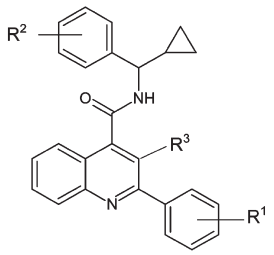

Cmpd	R^1	R^2	R^3	pKi (M)
3	H	H	NH_2	8.3
4	*m*-F	H	NH_2	8.0
5	H	*m*-F	NH_2	8.5
6*	H	*o*-F	NH_2	8.3
7	*m*-F	*m*-F	NH_2	8.2

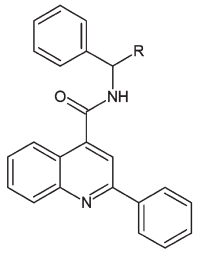

Cmpd	R	pKi (M)	Cmpd	R	pKi (M)
8	COOMe	7.5	**16**	i-Pr	7.1
9	CH_2COOMe	6	**17**	n-Bu	6.8
10	CONHMe	6.3	**18**	n-heptyl	5.3
11	$CONMe_2$	6.3	**19**	CH_2Ph	5.5
12	$CONH_2$	6	**20**	COMe	7.6
13	Me	6.6	**21**	CH_2OH	6.7
14*	Et	7.5	**22***	CH_2CH_2OH	6.4
15*	n-Pr	7.3	**23**	CF_3	6.3

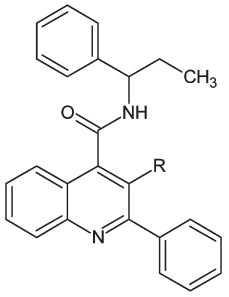

Cmpd	R	pKi (M)	Cmpd	R	pKi (M)
24*	Me	8	**29**	Ph	7.3
25	Et	8.2	**30**	OMe	8.2
26	n-Pr	7.9	**31**	OH	8.6
27	n-Bu	7.8	**32**	NH_2	8.7
28*	n-hexyl	7.3			

[a] * = test set.

obtained from suppliers and tested in vitro. The quinoline type compounds identified were first screened in the CoMFA model.

CoMFA Analysis. 3D-QSAR modeling was conducted using the CoMFA modules of SYBYL 8.1 (Tripos, St Louis MO) running on a Dell XPS720 3.66 GHz PC dual booted to run Red Hat Linux Enterprise 5 and Microsoft Windows XP. The aligned compounds from ROCS were used for the study. Gasteiger–Hückel charges were added to each before model development. The compounds were divided into a training set and a test set using the QSAR Wizard program for MOE (www.chemcomp.

com) which is available for download at the Chemical Computing group SVL exchange (http://svl.chemcomp.com/). The complete set was randomly divided irrespective of activity or chemical composition so that an 80% separation could be achieved, i.e., 80% of the set was designated as training set and 20% as test set. Few studies are available which have a large congeneric series of compounds related to talnetant that have binding data. We chose to use the training and test set presented in Table 5, the data for which came from NK_3 receptor binding assays.[6,11]

Default values were used with a 2.0 Å grid spacing using a sp^3 carbon atom with a +1 point charge as a probe to explore the steric and electrostatic interactions at the lattice points in the grid. The default cutoff value was set at 30 kcal/mol. Statistical analysis was performed using the partial least-squares (PLS) method implemented in the SYBYL program. Noncross-validated (r^2) values were determined for the models using linear regression analysis (with variances reported as the standard error of estimation, SEE) which are considered significant when r^2 is greater than 0.7. The q^2 values obtained were considered significant at 0.3, as per the developer's suggestion. The 3D graphical representation of the steric and electrostatic fields generated are shown with the relative contributions represented as a 3D coefficient map with favored 80% steric (green) and electrostatic (blue) effects and 20% disfavored steric (yellow) and electrostatic effects (red). Green colored areas of the map indicate where sterically bulky groups may enhance interaction affinity. Blue colored areas (80%) indicate regions where a more positively charged group will likely lead to increased binding affinity, while red areas indicate where a more negatively charged group will likely lead to increased binding (20%). Biological data were taken from literature[6,11] and entered as pK_i values. The pK_is ranged from 5.3 to 8.7. The model was used with these default methods, without further additional model validation, e.g. scrambling of data etc.

Compounds which were identified from the virtual screen and quinoline-based were then evaluated in the model to determine viability before undergoing binding and functional assays. Candidate compounds which were predicted to have an affinity of $< 10\ \mu M$ for binding to hNK_3Rs, and were available from the supplier as 1 mg stocks, were then analyzed in the binding and functional assays.

Receptor Binding: Competition Radioligand Binding. Membranes isolated from Chinese hamster ovary cells stably transfected with cDNA encoding the hNK_3R, provided by Dr. James E. Krause, ARMGO Pharma, Inc., Tarrytown, NY, were used to determine the competition binding properties of the compounds. [^{125}I]-MePhe^7-NKB, specific activity 2200 Ci/mmol, purchased from PerkinElmer (Boston, MA), at a concentration of 75 pM and increasing amounts, 10^{-12} to 10^{-5} M, of unlabeled compound, were used in the binding assays. The assay conditions used here are common competition radioligand binding conditions and have been used previously in our lab.[12−14] Briefly, membranes isolated from cells expressing the hNK_3R were incubated with [^{125}I]-MePhe^7-NKB and unlabeled test compound for 90 min at room temperature, washed to remove any unbound ligand, collected, and the radiation counted using a Packard Cobra II series auto-gamma counter (Packard, Meriden, CT).

Nonspecific binding (typically 200 dpm) was determined in the presence of 1 μM unlabeled MePhe^7-NKB. Specific binding was calculated by subtracting nonspecific binding from the total counts. Data points were normalized by dividing the specifically bound radiolabeled-MePhe^7-NKB counts in the presence of unlabeled peptide by the specifically bound radiolabeled-MePhe^7-NKB counts in the presence of the lowest concentration of test compound. Maximal specific binding under these conditions is < 5000 dpm. Data are plotted as the competitor concentration vs fraction specific binding. Each data point represents the mean ± standard error of the mean (SEM). The $n = 4-12$ for each point. Compounds used in these studies, were dissolved in DMSO, and control experiments used DMSO as vehicle control. Stock solutions were stored at −20 °C, with no apparent loss of activity.

Receptor Functional Assay: Calcium Signaling Assay. hNK_3R-expressing Chinese hamster ovary cells were maintained in α-MEM containing 10% FBS and 0.8 mg/mL G418. Cells were incubated on 24-well plates at 37 °C and 5% CO_2 for 3−4 days and grown to 80−90% confluency prior to use. On the day of the experiment, cells were rinsed 3× with extracellular solution, containing 1 mM $MgCl_2$, 5 mM KCl, 115 mM NaCl, 10 mM HEPES, 10 mM glucose, 2.3 mM $CaCl_2$, and 2.5 mM probenecid, pH 7.4, prior to being placed in a fluorescent plate-reader (Synergy H4, BioTek Instruments, Winooski, VT) at 37 °C. Extracellular solution supplemented with 1 μM Fluo 4-AM, a calcium indicator dye, and 0.1% Pluronic F-127 was added to the wells and uptake of the dye was allowed to proceed for 30 min. The cells were rinsed (3×) with extracellular solution just before measurement of intracellular calcium. The fluorescence emission at 520 nm following excitation at 485 nm was measured and used as an index of intracellular calcium levels. The fluorescence is measured in an area of 2.0 mm^2 in the center of each well. The number of cells within this area is 2000−3000. Triton X-100 (2.5%) was applied at the end of each experiment to obtain the maximum signal that was used to normalize the agonist-induced responses between samples. Data are expressed as a fraction of the maximal response (E_{max}) and include an n of 8 or more.

Concentration−response relationships for two NK_3R agonists, senktide and MePhe^7-NKB, were determined by applying graded concentrations ranging from 10^{-11} to 10^{-5} M to the wells and measuring the change in fluorescence. The EC_{50}s obtained were 100 nM for senktide and 25 nM for MePhe^7-NKB. Tests of antagonist compounds were conducted with agonist concentrations that gave approximately $^2/_3$ of the maximal calcium response (EC_{66}s), which are 200 nM for senktide and 50 nM for MePhe^7-NKB. For initial screening, the test compounds were applied at a concentration of 50 μM to the wells for 10 min prior to senktide application, and the effect on the response to senktide (200 nM) was tested. None of the compounds produced a detectable change in Ca fluorescence. Application of an equivalent volume of solvent without drug (extracellular solution with 0.1% DMSO) had no effect on basal fluorescence or the responses to senktide or MePhe^7-NKB.

References

(1) Spooren, W.; Riemer, C.; Meltzer, H. Opinion: NK3 receptor antagonists: the next generation of antipsychotics? *Nature Rev. Drug. Discovery* **2005**, *4*, 967–975.

(2) Regoli, D.; Boudon, A.; Fauchere, J. L. Receptors and antagonists for substance P and related peptides. *Pharm. Rev.* **1994**, *46*, 551–598.

(3) Meltzer, H. Y.; Stahl, S. M. The dopamine hypothesis of schizophrenia: a review. *Schizophr. Bull.* **1976**, *2*, 19–76.

(4) Meltzer, H. Y.; Arvanitis, L.; Bauer, D.; Rein, W. Placebo-controlled evaluation of four novel compounds for the treatment of schizophrenia and schizoaffective disorder. *Am. J. Psychiatry* **2004**, *161*, 975–984.

(5) Sarau, H. M.; Griswold, D. E.; Potts, W.; Foley, J. J.; Schmidt, D. B.; Webb, E. F.; Martin, L. D.; Brawner, M. E.; Elshourbagy, N. A.; Medhurst, A. D.; Giardina, G. A.; Hay, D. W. Nonpeptide tachykinin receptor antagonists: I. Pharmacological and pharmacokinetic characterization of SB 223412, a novel, potent and selective neurokinin-3 receptor antagonist. *J. Pharmacol. Exp. Ther.* **1997**, *281*, 1303–1311.

(6) Giardina, G. A.; Raveglia, L. F.; Grugni, M.; Sarau, H. M.; Farina, C.; Medhurst, A. D.; Graziani, D.; Schmidt, D. B.; Rigolio, R.; Luttmann, M.; Cavagnera, S.; Foley, J. J.; Vecchietti, V.; Hay, D. W. Discovery of a novel class of selective non-peptide antagonists for the human neurokinin-3 receptor. 2. Identification of (*S*)-*N*-(1-phenylpropyl)-3-hydroxy-2-phenylquinoline-4-carboxamide (SB 223412). *J. Med. Chem.* **1999**, *42*, 1053–1065.

(7) Agarwal, A.; Pearson, P. P.; Taylor, E. W.; Li, H. B.; Dahlgren, T.; Herslöf, M.; Yang, Y.; Lambert, G.; Nelson, D. L.; Regan, J. W.; Martin, A. R. Three-dimensional quantitative structure-activity relationships of 5-HT receptor binding data for tetrahydropyridinylindole derivatives: a comparison of the Hansch and CoMFA methods. *J. Med. Chem.* **1993**, *36*, 4006–4014.

(8) Tropsha, A.; Golbraikh, A. Predictive QSAR modeling workflow, model applicability domains, and virtual screening. *Curr. Pharm. Des.* **2007**, *13*, 3494–3504.
(9) Drapeau, G.; D'Orléans-Juste, P.; Dion, S.; Rhaleb, N. E.; Rouissi, N. E.; Regoli, D. Selective agonists for substance P and neurokinin receptors. *Neuropeptides* **1987**, *10*, 43–54.
(10) Irwin, J. J.; Shoichet, B. K. ZINC - A Free Database of Commercially Available Compounds for Virtual Screening. *J. Chem. Inf. Model.* **2005**, *45*, 177–182.
(11) Smith, P. W.; Wyman, P. A.; Lovell, P.; Goodacre, C.; Serafinowska, H. T.; Vong, A.; Harrington, F.; Flynn, S.; Bradley, D. M.; Porter, R.; Coggon, S.; Murkitt, G.; Searle, K.; Thomas, D. R.; Watson, J. M.; Martin, W.; Wu, Z.; Dawson, L. A. New quinoline NK3 receptor antagonists with CNS activity. *Bioorg. Med. Chem. Lett.* **2009**, *19*, 837–840.
(12) Bennett, V. J.; Simmons, M. A. Analysis of fluorescently-labeled substance P analogs: binding, imaging and receptor activation. *BMC Chem. Biol.* **2001**, *1* (1), 12.
(13) Simmons, M. A. Functional selectivity of NK1 receptor signaling: Peptide agonists can preferentially produce receptor activation or desensitization. *J. Pharmacol. Exp. Ther.* **2006**, *319*, 907–913.
(14) Perrine, S. A.; Beard, D. J.; Young, J.; Simmons, M. A. The role of the N-terminal and mid-region residues of substance P in regulating functional selectivity at the NK1 receptor. *Eur. J. Pharmacol.* **2008**, *592*, 1–6.